Methanol-to-Hydrocarbons

International Edition: DOI: 10.1002/anie.201803279
German Edition: DOI: 10.1002/ange.201803279

# Bridging the Gap between the Direct and Hydrocarbon Pool Mechanisms of the Methanol-to-Hydrocarbons Process

*Abhishek Dutta Chowdhury, Alessandra Lucini Paioni, Klaartje Houben, Gareth T. Whiting, Marc Baldus, and Bert M. Weckhuysen**

***Abstract:*** *After a prolonged effort over many years, the route for the formation of a direct carbon–carbon (C–C) bond during the methanol-to-hydrocarbon (MTH) process has very recently been unveiled. However, the relevance of the "direct mechanism"-derived molecules (that is, methyl acetate) during MTH, and subsequent transformation routes to the conventional hydrocarbon pool (HCP) species, are yet to be established. This important piece of the MTH chemistry puzzle is not only essential from a fundamental perspective, but is also important to maximize catalytic performance. The MTH process was probed over a commercially relevant H-SAPO-34 catalyst, using a combination of advanced solid-state NMR spectroscopy and operando UV/Vis diffuse reflectance spectroscopy coupled to an on-line mass spectrometer. Spectroscopic evidence is provided for the formation of (olefinic and aromatic) HCP species, which are indeed derived exclusively from the direct C–C bond-containing acetyl group of methyl acetate. New mechanistic insights have been obtained from the MTH process, including the identification of hydrocarbon-based co-catalytic organic reaction centers.*

Overall, carbon emissions from renewable feedstocks such as biomass and waste, are significantly lower than from fossil resources.[1] Thus, the methanol-to-hydrocarbons (MTH) process over zeolites is arguably one of the most sustainable pathways to produce liquid transportation fuels as well as $C_2$–$C_4$ olefins from renewable resources (provided the methanol is not sourced from natural gas/coal).[2–5] Despite the industrial success of the MTH process, it is a highly complicated reaction mechanistically, which has led to the proposal of over twenty different mechanisms over the last three decades.[6] Surprisingly, the exact route for the formation of a direct carbon–carbon (C–C) bond from methanol has very recently been recognized.[7–17] Previously, the presence of trace impurities (for example, in the methanol, catalyst, and/or carrier gas) were thought to be responsible for the formation of the initial C–C bonds by the direct mechanism.[18,19] This assumption resulted from a lack of concrete experimental support, as well as theoretical calculations that predicted the direct mechanism was unrealistic (that is, higher activation barriers and/or unstable intermediates).[20] In 2006, Hunger et al. systematically rejected the proposal that impurities play an influential role by demonstrating that they do not affect the formation of the initial hydrocarbon pool (HCP) species.[13] Subsequently, different research groups (for example, Kondo, Fan, Copéret, Lercher, Liu, and Studt), including our own, have delivered both experimental and theoretical evidence in support of the existence of a direct mechanism during the early stages of the MTH process.[7–17]

Among several direct coupling proposals, the Koch-type carbonylation mechanism is now the most widely acknowledged route to form direct C–C bonds in the MTH process (Scheme 1).[7,10,16] Lercher and coworkers proposed that methyl acetate ($CH_3CO_2CH_3$ derived by carbonylation of methanol) is the very first C–C bond-containing species during the MTH reaction over zeolite H-ZSM-5.[10] Shortly afterwards, we provided vital spectroscopic evidence in support of the Koch-type carbonylation route during the MTH reaction over H-SAPO-34.[7] Very recently, this proposal for Koch-type carbonylation by a direct mechanism was theoretically verified by Plessow and Studt.[16,17] In this mechanism, a surface methoxy species (SMS) is first formed upon adsorption of methanol onto a Brønsted acid site of the

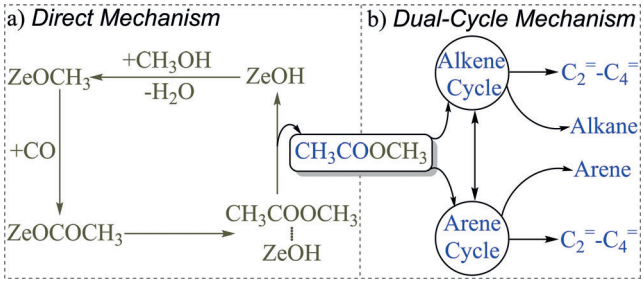


***Scheme 1.*** Simplified mechanistic illustration of the methanol-to-hydrocarbon (MTH) process catalyzed by zeolite (denoted as ZeOH), comprising a) Koch-type carbonylation direct and b) hydrocarbon pool (HCP)/dual-cycle mechanisms. Selective isotope ($^{13}C$) labeling of the (direct C–C bond-containing) acetyl group of methyl acetate (denoted in blue) permitted specific study of the governing co-catalytic organic reaction centers in the HCP mechanism of the MTH process.

[*] Dr. A. D. Chowdhury, Dr. G. T. Whiting, Prof. Dr. B. M. Weckhuysen
Inorganic Chemistry and Catalysis Group, Debye Institute for Nanomaterials Science, Utrecht University
Universiteitsweg 99, 3584 CG Utrecht (The Netherlands)
E-mail: b.m.weckhuysen@uu.nl
A. L. Paioni, Dr. K. Houben, Prof. Dr. M. Baldus
NMR Spectroscopy group, Bijvoet Center for Biomolecular Research
Utrecht University
Padualaan 8, 3584 CH Utrecht (The Netherlands)
Dr. K. Houben
Current address: DSM Food Specialties, DSM Biotechnology Center R&D analysis
Alexander Flemminglaan 1, 2613 AX Delft (The Netherlands)
Supporting information and the ORCID identification number(s) for the author(s) of this article can be found under: https://doi.org/10.1002/anie.201803279.

zeolite (Scheme 1 a).[7,12,16,17] Subsequently, SMS undergoes carbonylation (through dehydrogenation of methanol/formaldehyde) to form direct C–C bond-containing surface acetate species.[7,10,16,17] The surface acetate species lead to the formation of methyl acetate (Scheme 1 a), which independently initiates the formation of HCP species and $C_2$–$C_4$ olefins (Scheme 1 b).[7,16,17] All three responsible intermediates in this carbonylation-based mechanism (SMS, zeolite-acetate, and methyl acetate) were previously characterized by our group spectroscopically.[7] However, the influential HCP species in the autocatalytic dual-cycle mechanism, which could be derived directly from the methyl acetate, are yet to be identified. This could be an essential piece of information within MTH chemistry, and is considered mechanistically necessary for connecting the direct and HCP mechanisms.

From a different perspective, our earlier proposed Koch-type carbonylation direct mechanism for the MTH reaction (Scheme 1 a) has conceptual resemblance to the Monsanto and BP's Cativa® processes (that is, to form acetic acid/methyl acetate from methanol/dimethyl ether (DME)).[21–24] Although industry currently uses Rh/Ir organometallic catalysts for this process, zeolites have recently appeared as an alternative option to overcome existing disadvantages (for example, non-recyclability of expensive catalysts, tedious separation steps, and the use of corrosive water-insoluble additives).[23] Thus, mechanistic understanding of the fate of methyl acetate over zeolite-based materials will also be beneficial for unravelling other zeolite-catalyzed hydrocarbon conversion processes.

In this context, the primary objective of this work is to shed light onto the hydrocarbon-based "co-catalytic" reaction centers in the autocatalytic part of the MTH reaction, that are exclusively derived from the direct C–C bond-containing acetyl group of methyl acetate. These ambitions were realized through the identification of the governing HCP species (for example, carbonylates, olefins, aromatics, and alkanes), during the methyl-acetate-to-hydrocarbon (MATH) reaction over H-SAPO-34. By encompassing advanced magic-angle spinning (MAS) solid-state nuclear magnetic resonance (NMR) spectroscopy and operando UV/Vis diffuse reflectance spectroscopy (DRS) coupled with on-line mass spectrometry (MS), such in-depth information of the reaction mechanism could be obtained. This study further reinforces the concept of the hybrid inorganic–organic nature of the catalyst material, where the mobility-dependent distinct host–guest chemistry between the zeolite and the trapped hydrocarbons plays an important role.

Initially, operando UV/Vis DRS with on-line MS was employed to differentiate between neutral and carbenium HCP species, as well as to identify gas-phase products in the effluent gas stream during the MATH reaction over H-SAPO-34 at 673 K for 30 minutes (Supporting Information, Section SI, Figure S1).[7] The observed bands at approximately 297, 350, 419, and 624 nm were attributed to the neutral methylated benzenes, dienylic carbocationic/methylbenzenium ions, trienylic/highly methylated arenium ions, and methylated poly-arenium ions/highly conjugated polyenes, respectively (Supporting Information, Figures S1a–d).[7,14,25] Interestingly, the MS data of this reaction, as presented in Figure S1e–f (Supporting Information), reveals predominance of methane, methanol, DME, dimethoxymethane, ethylene, and propylene in the effluent gas stream, as well as butylene and tetramethylethylene (or a structural isomer of $C_6H_{12}$) in a lower quantity.[7]

Subsequently, we conducted solid-state NMR experiments on H-SAPO-34 after exposure to the MATH reaction for 30 minutes at 673 K using [1,2-$^{13}C_2$]methyl acetate ($^{13}CH_3{}^{13}CO_2{}^{12}CH_3$). Such selective isotope enrichment on the acetyl group not only enhanced NMR signal intensities, but also allowed us to perform multidimensional solid-state NMR correlation experiments to probe the molecular structures of zeolite-trapped organic reaction centers, which originated exclusively from the (direct C–C bond-containing) acetyl group (Supporting Information, Tables S1 and S2). The $^1$H-$^{13}$C cross-polarization (CP),[26] $^1$H-$^{13}$C insensitive nuclei enhanced by polarization transfer (INEPT),[27] and $^{13}$C direct excitation (DE) solid-state NMR spectra of the post-reacted catalyst are presented in Figure 1. The following three features were primarily observed: 1) 7–50 ppm aliphatic and methyl groups, 2) 120–160 ppm (methylated) aromatic/olefinic groups, and 3) 175–190 ppm carbonyl groups (Supporting Information, Table S1). The strongest aliphatic and aromatic signals at 18–22 and 127–136 ppm, respectively, contain contributions from the zeolite-trapped methylated benzene/olefinic molecules, consistent with the dual-cycle/HCP species.

To elucidate the molecular structures of the catalyst trapped species in more detail, we performed several 2D solid-state NMR experiments (Figures 2 and 3; Supporting Information, Figures S2 and S3), which allowed us to spectrally resolve different molecules on the basis of their mobility. As described in our previous work,[7,28–30] it is possible to identify species with high or low mobility by applying either through-bond (scalar interactions such as in

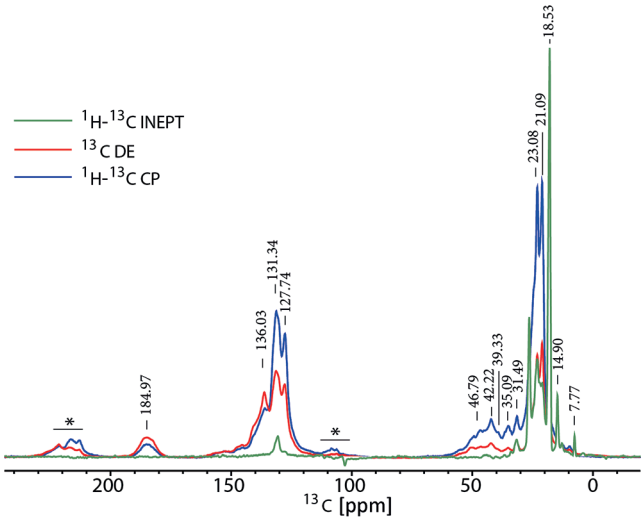


***Figure 1.*** 1D $^{13}$C spectra of molecules trapped by H-SAPO-34, with $^1$H-$^{13}$C CP (blue, 15 kHz MAS, NS = 4k), $^{13}$C DE (red, 15 kHz MAS, NS = 4k), and $^1$H-$^{13}$C INEPT (green, 15 kHz MAS, NS = 8k) solid-state NMR spectra of trapped products obtained after the [1,2-$^{13}C_2$]methyl-acetate-to-hydrocarbon reaction for 30 minutes at 673 K. Key: spinning sideband (*), magic-angle spinning (MAS), number of scans (NS).

  

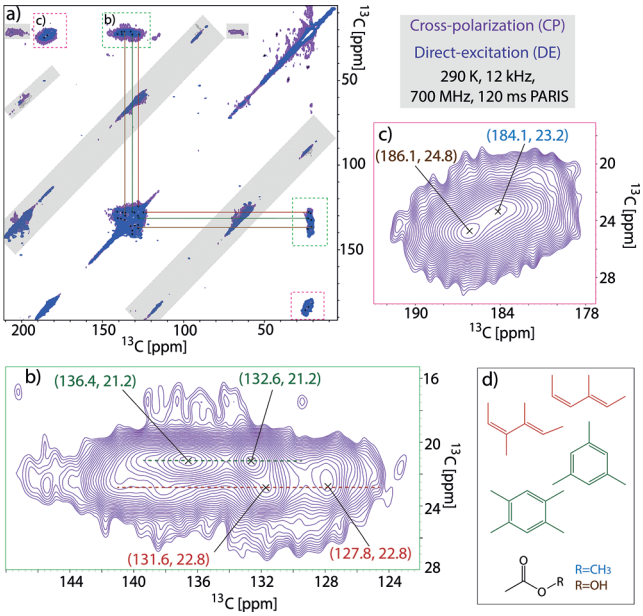


***Figure 2.*** a) 2D $^{13}C$-$^{13}C$ MAS solid-state NMR spectra of rigid molecules (290 K, 12 kHz, 700 MHz). Polarization of $^{13}C$ atoms was achieved through cross-polarization (CP, purple) or direct excitation (DE, blue) and a 120 ms PARIS mixing period was used. Gray filled regions indicate spinning side bands. b) Expansion of the aromatic/olefinic signals from the 2D $^{13}C$-$^{13}C$ CP MAS solid-state NMR spectrum. c) Expansion from the 2D $^{13}C$-$^{13}C$ CP MAS solid-state NMR spectrum, indicating acetic acid and methyl acetate resonances. d) Identified generic molecular keys/structures.

INEPT)[27] or through-space (dipolar transfer such as in CP)[26] magnetization transfer schemes, respectively. As a result, we could distinguish both mobile (that is, molecules/groups with fast tumbling or rotation) and rigid (that is, molecules physisorbed in/on zeolite) versions of zeolite-trapped organics after the MATH reaction. Additionally, DE experiments were performed to excite all chemical species, including those that exhibit intermediate dynamics (for which either an INEPT or CP transfer would be less efficient).[29] Therefore, unsaturated molecules (olefin/aromatics/carbonyls) were found to be either immobilized (compare CP in Figure 1) or have restricted mobility (compare DE in Figure 1). In contrast, mobile molecules were predominantly saturated/aliphatic in nature (compare INEPT in Figure 1).

To probe rigid molecules, we acquired 2D $^{13}C$-$^{13}C$ correlation spectra (Figure 2; Supporting Information, Figure S2). The carbon nuclei were polarized either through CP (purple) or DE (blue) and $^{13}C$–$^{13}C$ mixing was achieved through proton-driven spin diffusion (PDSD) using phase alternated recoupling irradiation schemes (PARIS).[31] The same set of molecules were visible in both spectra and clear correlations were observed between aliphatic/methyl groups and aromatic/olefinic moieties, unambiguously proving that the acetyl group of the methyl acetate was indeed incorporated into (methylated) aromatic and olefinic compounds (Figure 2a). Even though the assignment of the peaks is not straightforward (because of spectral crowding), the presence of molecules, such as 3-methyl/3,4-dimethylhexa-2,4-diene (alkene cycle species) and 1,3,5-tri/1,2,4,5-tetramethylbenzene (arene cycle species), were compatible with the correlations between signals in the 21–23 ppm and 130–140 ppm regions (Figures 2b,d; Supporting Information, Figure S2b). Moreover, in the carbonyl region, the signals at 184.1 and 186.1 ppm exhibited cross-peaks with a $^{13}C$ methyl signal at 23.2 and 24.8 ppm, respectively, which we attributed to the methyl acetate (the reactant) and acetic acid, respectively (Figures 2c,d; for surface acetate species see the Supporting Information, Figure S3). Interestingly, the linewidths of the rigid molecules observed in the CP-based spin diffusion spectra are significantly broader than that seen in the DE-based spectra (Supporting Information, Figure S2), possibly indicating that the same molecule exists in different molecular environments inside the zeolite framework, and surface-absorbed (less mobile) molecules are more enhanced in CP-based experiments.

Additionally, we detected mobile molecules (Figure 3), the hydrogen-transferred species from olefins (that is, $C_2$–$C_6$ alkanes) using 2D solid-state NMR measurements that invoke homonuclear through-bond transfer. Here, $^{13}C$-$^{13}C$ mixing was achieved by total through-bond correlation spectroscopy (TOBSY) transfer.[32] In the $^{13}C$-$^{1}H$ correlation spectrum, ethane (7.7 ($^{13}C$) and 0.73 ($^{1}H$) ppm) and propane (18.6 ($^{13}C$)/1.2 ($^{1}H$) and 18.0 ($^{13}C$)/0.79 ($^{1}H$) ppm) signals were readily identified. On combining $^{13}C$-$^{13}C$ and $^{13}C$-$^{1}H$

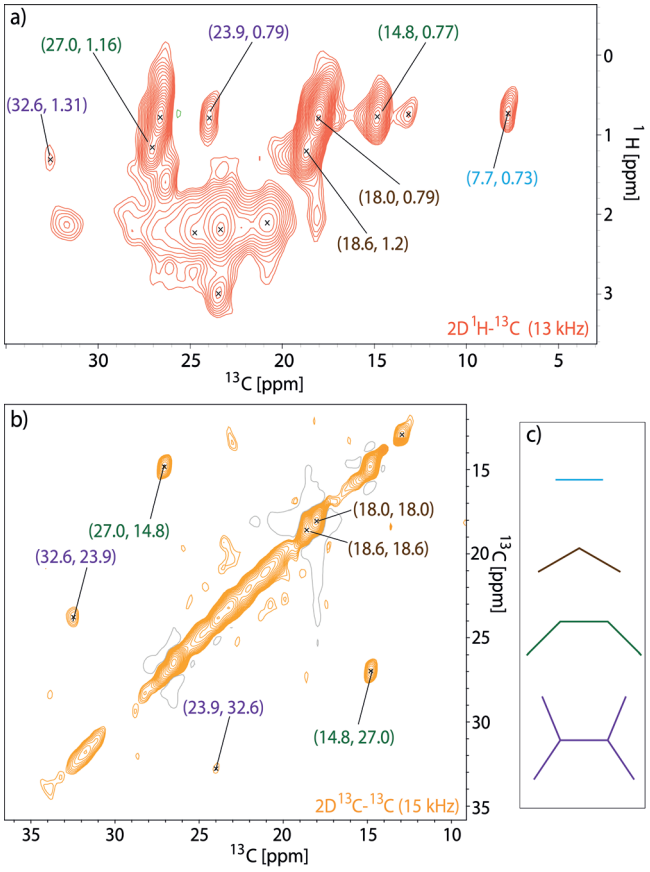


***Figure 3.*** 2D a) $^{13}C$-$^{1}H$ and b) $^{13}C$-$^{13}C$ MAS solid-state NMR correlation experiments probing the c) mobile molecules (measurement parameters: 266 K, 13 kHz, 700 MHz (a); 290 K, 15 kHz, 700 MHz (b)). In (b) a TOBSY mixing time of 4.3 ms was used.

correlation experiments, butane and tetramethylethane were distinguished as well (Figure 3; Supporting Information, Table S1).

Based on the aforementioned results, a catalytic pathway for the MATH reaction over H-SAPO-34 is proposed in Scheme 2. Firstly, methyl acetate (**A**) interacts with the zeolite (**B**) to form surface acetate species (**C**) by acetylation

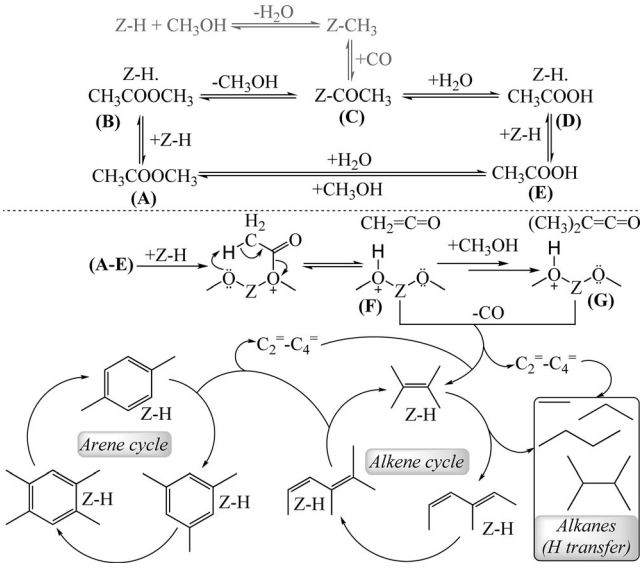


***Scheme 2.*** Proposed reaction pathways of the methyl-acetate-to-hydrocarbon (MATH) conversion catalyzed by zeolite (denoted as Z-H).

of Brønsted acid sites of the zeolite. Simultaneously, **C** could be hydrolyzed to form both rigid (**D**, that is, zeolite adduct) and mobile (**E**) versions of acetic acid. The existence of the Koch-type carbonylation-based direct C–C bond-forming mechanistic route from methanol during the early stages of the MTH process was previously suggested independently by the groups of Jackson[33] and Hirao.[34] In this regard, recently Plessow and Studt also suggested that ketene ($CH_2CO$ in **F**) was formed from the acetyl moiety ($CH_3CO^+$ in **A**–**E**).[16,17] Notably, ketene belongs to the first generation of highly reactive intermediates and synthons in organic chemistry.[35] In the vicinity of Brønsted acidic sites, an acetyl group is nothing but a physisorbed protonated ketene (that is, $CH_2CO + H^+ \rightarrow CH_3CO^+$, with a very small energy barrier of $\leq 17\,kJ\,mol^{-1}$ and a large energy gain of $> 50\,kJ\,mol^{-1}$).[16,24,36] Thus, the steady-state concentration of ketene is not only low (particularly at the higher reaction temperature), but its existing rapid equilibrium to acetyl might fundamentally prohibit its direct detection by experimental methods in the present study.[24,36,33,37] It is worth mentioning that ketene was experimentally observed previously, during the conversion of syngas to light olefins by Fischer–Tropsch synthesis using bifunctional catalysts.[38] In the present case, the identification of acetic acid could be considered as indirect support for the existence of ketene ($CH_2CO + H_2O \rightarrow CH_3CO_2H$).[24] Moreover, the existence of ketene during the zeolite-catalyzed Koch-type carbonylation was hitherto theoretically predicted by multiple research groups.[16,17,24,33–35,39] Thus, $C_2$–$C_4$ olefins were initially formed by decarbonylation of ketenes, as proposed by Plessow and Studt (**F**/**G** in Scheme 2; Supporting Information, Figure S1).[16,17] Subsequently, smaller olefins oligomerize into bigger olefinic and aromatic species as a part of the alkene and arene cycle of the dual-cycle/HCP mechanism, respectively, to govern the autocatalytic part of the reaction.[16,17] Moreover, these identified HCP species were already established as co-catalysts in the corresponding cycles during the autocatalysis period.[40–42] Therefore, this work not only accurately elucidates structures of the co-catalytic HCP species, but also further supports the founding postulation of Svelle et al. in which a hybrid inorganic–organic material is proposed as the active MTH catalyst (that is, a catalyst comprising the inorganic zeolite and organic HCP reaction centers).[42] Finally, simultaneous detection of $C_2$–$C_6$ alkanes also confirms that the production of olefin and hydrogen-transferred products (that is, alkanes/arenes) occurred in parallel (rather than sequential) reaction pathways (Scheme 2, Figure 3).[40,43,44] Thus, homologation of olefins, cracking of olefins/aromatics, and hydrogen transfer, were identified as three predominant reactions in this chemistry (Scheme 2).[40]

In conclusion, the present work clearly demonstrates that the direct C–C bond-forming route (that is, a direct mechanism during the zeolite-catalyzed MTH process) is indeed responsible for the initial formation of certain HCP-type organic reaction centers, which were considered as co-catalysts in the autocatalytic part of the reaction. Three types of HCP species (that is, olefins, arenes, and alkanes) have been recognized with unprecedented clarity, which were derived exclusively from the directly formed C–C bond-containing acetyl group. Moreover, the nature of the hybrid inorganic–organic working MTH catalyst material was explored, including its mobility-dependent features. The acquired knowledge not only provides a clear blueprint to upgrade the existing MTH technology (by either stimulating or suppressing one cycle over the other in the dual-cycle mechanism to yield a desired hydrocarbon range from methanol), but can also contribute to the basic understanding of zeolite-catalyzed hydrocarbon conversion chemistry.

## Acknowledgements

This project has received funding from the European Union's Horizon 2020 research and innovation program under the Marie Skłodowska-Curie grant agreement (no. 704544 to A.D.C.), an European Research Council Advanced Grant (no. 321140 to B.M.W.), a Veni grant (no. 722.015.003 to G.T.W.), and a Middelgroot program (no. 700.58.102 to M.B.). K.H. was supported by uNMR-NL, an NWO-funded National Roadmap Large-Scale Facility for the Netherlands (no. 184.032.207). Authors thank Katarína Stančiaková (Utrecht University) for the preparation of the TOC image.

  

## Conflict of interest

The authors declare no conflict of interest.

**Keywords:** heterogeneous catalysis · hydrocarbon pool · reaction mechanisms · solid-state NMR · zeolites


[1] B. Walsh, P. Ciais, I. A. Janssens, J. Peñuelas, K. Riahi, F. Rydzak, D. P. van Vuuren, M. Obersteiner, *Nat. Commun.* **2017**, *8*, 14856.
[2] U. Olsbye, S. Svelle, K. P. Lillerud, Z. H. Wei, Y. Y. Chen, J. F. Li, J. G. Wang, W. B. Fan, *Chem. Soc. Rev.* **2015**, *44*, 7155 – 7176.
[3] P. Tian, Y. Wei, M. Ye, Z. Liu, *ACS Catal.* **2015**, *5*, 1922 – 1938.
[4] S. Ilias, A. Bhan, *ACS Catal.* **2013**, *3*, 18 – 31.
[5] U. Olsbye, S. Svelle, M. Bjrgen, P. Beato, T. V. W. Janssens, F. Joensen, S. Bordiga, K. P. Lillerud, *Angew. Chem. Int. Ed.* **2012**, *51*, 5810 – 5831; *Angew. Chem.* **2012**, *124*, 5910 – 5933.
[6] M. Stöcker, *Microporous Mesoporous Mater.* **1999**, *29*, 3 – 48.
[7] A. D. Chowdhury, K. Houben, G. T. Whiting, M. Mokhtar, A. M. Asiri, S. A. Al-Thabaiti, M. Baldus, B. M. Weckhuysen, *Angew. Chem. Int. Ed.* **2016**, *55*, 15840 – 15845; *Angew. Chem.* **2016**, *128*, 16072 – 16077.
[8] H. Yamazaki, H. Shima, H. Imai, T. Yokoi, T. Tatsumi, J. N. Kondo, *Angew. Chem. Int. Ed.* **2011**, *50*, 1853 – 1856; *Angew. Chem.* **2011**, *123*, 1893 – 1896.
[9] A. Comas-Vives, M. Valla, C. Copéret, P. Sautet, *ACS Cent. Sci.* **2015**, *1*, 313 – 319.
[10] Y. Liu, S. Müller, D. Berger, J. Jelic, K. Reuter, M. Tonigold, M. Sanchez-Sanchez, J. A. Lercher, *Angew. Chem. Int. Ed.* **2016**, *55*, 5723 – 5726; *Angew. Chem.* **2016**, *128*, 5817 – 5820.
[11] X. Wu, S. Xu, W. Zhang, J. Huang, J. Li, B. Yu, Y. Wei, Z. Liu, *Angew. Chem. Int. Ed.* **2017**, *56*, 9039 – 9043; *Angew. Chem.* **2017**, *129*, 9167 – 9171.
[12] W. Wang, M. Hunger, *Acc. Chem. Res.* **2008**, *41*, 895 – 904.
[13] Y. Jiang, W. Wang, V. Reddymarthala, J. Huang, B. Sulikowski, M. Hunger, *J. Catal.* **2006**, *238*, 21 – 27.
[14] W. Dai, C. Wang, M. Dyballa, G. Wu, N. Guan, L. Li, Z. Xie, M. Hunger, *ACS Catal.* **2015**, *5*, 317 – 326.
[15] J. Li, Z. Wei, Y. Chen, B. Jing, Y. He, M. Dong, H. Jiao, X. Li, Z. Qin, J. Wang, W. Fan, *J. Catal.* **2014**, *317*, 277 – 283.
[16] P. N. Plessow, F. Studt, *ACS Catal.* **2017**, *7*, 7987 – 7994.
[17] P. N. Plessow, F. Studt, *Catal. Lett.* **2018**, *148*, 1246 – 1253.
[18] I. M. Dahl, S. Kolboe, *Catal. Lett.* **1993**, *20*, 329 – 336.
[19] W. Song, D. M. Marcus, H. Fu, J. O. Ehresmann, J. F. Haw, *J. Am. Chem. Soc.* **2002**, *124*, 3844 – 3845.
[20] D. Lesthaeghe, V. Van Speybroeck, G. B. Marin, M. Waroquier, *Ind. Eng. Chem. Res.* **2007**, *46*, 8832 – 8838.
[21] P. Cheung, A. Bhan, G. J. Sunley, E. Iglesia, *Angew. Chem. Int. Ed.* **2006**, *45*, 1617 – 1620; *Angew. Chem.* **2006**, *118*, 1647 – 1650.
[22] M. Boronat, C. Martínez-Sánchez, D. Law, A. Corma, *J. Am. Chem. Soc.* **2008**, *130*, 16316 – 16323.
[23] C. Le Berre, P. Serp, P. Kalck, G. P. Torrence, C. Le Berre, P. Serp, P. Kalck, G. P. Torrence in *Ullmann's Encyclopedia of Industrial Chemistry*, Wiley-VCH, Weinheim, **2014**, pp. 1 – 34.
[24] D. B. Rasmussen, J. M. Christensen, B. Temel, F. Studt, P. G. Moses, J. Rossmeisl, A. Riisager, A. D. Jensen, *Angew. Chem. Int. Ed.* **2015**, *54*, 7261 – 7264; *Angew. Chem.* **2015**, *127*, 7369 – 7372.
[25] M. J. Wulfers, F. C. Jentoft, *ACS Catal.* **2014**, *4*, 3521 – 3532.
[26] A. Pines, M. G. Gibby, J. S. Waugh, *J. Chem. Phys.* **1973**, *59*, 569 – 590.
[27] G. A. Morris, R. Freeman, *J. Am. Chem. Soc.* **1979**, *101*, 760 – 762.
[28] O. C. Andronesi, S. Becker, K. Seidel, H. Heise, H. S. Young, M. Baldus, *J. Am. Chem. Soc.* **2005**, *127*, 12965 – 12974.
[29] A. D. Chowdhury, K. Houben, G. T. Whiting, S.-H. Chung, M. Baldus, B. M. Weckhuysen, *Nat. Catal.* **2018**, *1*, 23 – 31.
[30] T. Blasco, *Nat. Catal.* **2018**, *1*, 8 – 9.
[31] M. Weingarth, D. E. Demco, G. Bodenhausen, P. Tekely, *Chem. Phys. Lett.* **2009**, *469*, 342 – 348.
[32] M. Baldus, B. H. Meier, *J. Magn. Reson. Ser. A* **1996**, *121*, 65 – 69.
[33] J. E. Jackson, F. M. Bertsch, *J. Am. Chem. Soc.* **1990**, *112*, 9085 – 9092.
[34] N. Tajima, T. Tsuneda, F. Toyama, K. Hirao, *J. Am. Chem. Soc.* **1998**, *120*, 8222 – 8229.
[35] R. Miller, C. Abaecherli, A. Said, B. Jackson, R. Miller, C. Abaecherli, A. Said, B. Jackson, *Ketenes in Ullmann's Encyclopedia of Industrial Chemistry*, Wiley-VCH, Weinheim, **2001**.
[36] D. E. Resasco, B. Wang, S. Crossley, *Catal. Sci. Technol.* **2016**, *6*, 2543 – 2559.
[37] G. Hutchings, *J. Catal.* **1993**, *142*, 602 – 616.
[38] F. Jiao, J. Li, X. Pan, J. Xiao, H. Li, H. Ma, M. Wei, Y. Pan, Z. Zhou, M. Li, S. Miao, J. Li, Y. Zhu, D. Xiao, T. He, J. Yang, F. Qi, Q. Fu, X. Bao, *Science* **2016**, *351*, 1065 – 1068.
[39] A. D. Allen, T. T. Tidwell, *Chem. Rev.* **2013**, *113*, 7287 – 7342.
[40] X. Sun, S. Mueller, Y. Liu, H. Shi, G. L. Haller, M. Sanchez-Sanchez, A. C. Van Veen, J. A. Lercher, *J. Catal.* **2014**, *317*, 185 – 197.
[41] M. Bjørgen, S. Svelle, F. Joensen, J. Nerlov, S. Kolboe, F. Bonino, L. Palumbo, S. Bordiga, U. Olsbye, *J. Catal.* **2007**, *249*, 195 – 207.
[42] S. Svelle, F. Joensen, J. Nerlov, U. Olsbye, K.-P. Lillerud, S. Kolboe, M. Bjørgen, *J. Am. Chem. Soc.* **2006**, *128*, 14770 – 14771.
[43] S. Müller, Y. Liu, F. M. Kirchberger, M. Tonigold, M. Sanchez-Sanchez, J. A. Lercher, *J. Am. Chem. Soc.* **2016**, *138*, 15994 – 16003.
[44] J. S. Martínez-Espín, K. De Wispelaere, T. V. W. Janssens, S. Svelle, K. P. Lillerud, P. Beato, V. Van Speybroeck, U. Olsbye, *ACS Catal.* **2017**, *7*, 5773 – 5780.


Manuscript received: March 17, 2018
Revised manuscript received: April 23, 2018
Accepted manuscript online: April 30, 2018
Version of record online: ■■ ■■, ■■■■

  

# Communications

**Methanol-to-Hydrocarbons**

A. D. Chowdhury, A. L. Paioni, K. Houben, G. T. Whiting, M. Baldus, B. M. Weckhuysen* _____ ▮▮▮▮–▮▮▮▮

Bridging the Gap between the Direct and Hydrocarbon Pool Mechanisms of the Methanol-to-Hydrocarbons Process

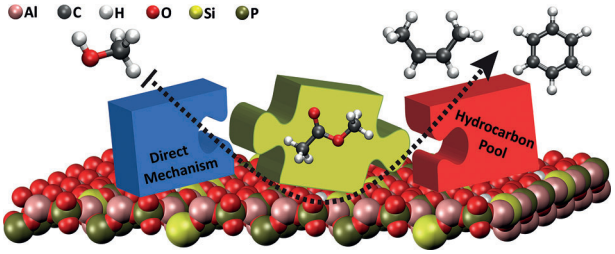


**Like a MTH to a flame**: The direct mechanism for the zeolite-catalyzed methanol-to-hydrocarbon (MTH) process directly generates co-catalytic hydrocarbon reaction centers in the hydrocarbon pool. Advanced solid-state NMR spectroscopy, mass spectrometry, and UV/Vis diffuse reflectance spectroscopy provide evidence for the formation of olefinic and aromatic species in the hydrocarbon pool.

  